ChemistrySelect

Research Article
doi.org/10.1002/slct.202203560

Chemistry Europe
European Chemical Societies Publishing

www.chemistryselect.org

Special Collection

Design of a Novel Naphtiridine-based Covalent Triazine Framework for Carbon Dioxide Capture and Storage Applications

Giulia Tuci,*[a] Matteo Pugliesi,[a] Andrea Rossin,[a] Cuong Pham-Huu,[b] Enrico Berretti,[a] and Giuliano Giambastiani[a, b]

In memory of our colleague Lapo Luconi (1978-2020), a beloved and unforgettable friend.

Covalent triazine frameworks (CTFs) represent a sub-class of Porous Organic Polymers showing high chemical/thermal stability, large permanent porosity and intrinsically high N-content. All these features make them ideal candidates for Carbon Capture and Storage (CCS) applications. Herein, a novel CTF has been prepared under ionothermal conditions through cyclotrimerization of a newly designed dicyano-building block with high N/C ratio (2,6-Dicyano-1,5-naphthyridine, **4**). The as prepared **CTF-Napht** showed remarkable carbon dioxide uptake at ambient conditions, with a loading of 3.93 mmol/g (17.3 wt.%) at 1 bar and 298 K that outperforms many benchmark CTF systems from the literature. The *ad-hoc* designed dicyano building unit together with a judicious choice of synthetic conditions have imparted to **CTF-Napht** an outstanding affinity towards CO_2 confirmed by its isosteric heat of adsorption (Q_{st}) as high as 39.6 KJ/mol that ranks among the highest reported so far for CTF-based polymers.

Introduction

One of the most urgent priorities of modern society is the mitigation of detrimental effects of global warming, mainly caused by uncontrolled anthropogenic CO_2 emissions in the atmosphere.[1] Albeit intense research efforts towards an efficient exploitation of renewable sources for clean energy production are being made worldwide, nowadays fossil fuels still play a primary role for fulfilling the global energy demand. As a result, CO_2 levels in the atmosphere are steadily growing, reaching the present worrying threshold of 421 ppm.[2] While we are waiting for a desirable global revolution towards a sustainable and low carbon footprint society, a readily available alternative is the sequestration of atmospheric CO_2 *via* the Carbon Capture and Storage (CCS) approach.[3] On this ground, CO_2 physisorption in highly porous materials at ambient temperature (physical storage) represents a more convenient alternative to traditional energy consuming amine-based scrubbing (chemical storage) or cryogenic condensation methods.[4]

Covalent triazine frameworks (CTFs), first introduced in 2008 by Thomas and co-workers,[5] are a subclass of Porous Organic Polymers (POPs) presenting high chemical and thermal stability together with high SSA and permanent porosity that make them ideal candidates for gas storage applications.[6] CTFs are classically synthesized through cyclotrimerization of dicyanoaryl compounds under ionothermal conditions. The experimental synthetic conditions deeply influence the materials final texture (SSA, porosity, crystallinity) and chemical composition (N-content, surface polarity).[5,7–9] As a result, different trimerization conditions as well as the virtually infinite set of available dicyano building blocks have paved the way for the design of a large variety of CTFs with a broad range of morphological and chemico-physical properties conveniently tunable on the basis of their downstream applications.[10–11]

With the aim at promoting CO_2 adsorption, a common strategy relies on the insertion of basic functional groups in the dicyano building unit in order to enhance the material affinity for (acidic) CO_2. CTFs high N-content has been found to boost the interaction with CO_2 ensuring remarkable adsorption performance.[12] In particular, a wide range of N-rich frameworks has been prepared starting from pyridine-,[13] imidazole-,[14] pyrimidine-, lutidine- and bypiridine-[15] based dinitriles. These studies investigated the influence of various parameters on the materials final CO_2 uptake capacity; the collected results unveiled that the adsorption performance is a delicate balance among the overall N-content, SSA and microporosity. High trimerization temperatures (*i.e.* 700–750 °C) generate materials with high surface area and pore volume but featured by a

[a] *Dr. G. Tuci, M. Pugliesi, Dr. A. Rossin, Dr. E. Berretti, Dr. G. Giambastiani*
Institute of Chemistry of OrganoMetallic Compounds,
ICCOM-CNR and Consorzio INSTM,
Via Madonna del Piano, 10, 50019 Sesto F.no, Florence, Italy
E-mail: giulia.tuci@iccom.cnr.it
[b] *Dr. C. Pham-Huu, Dr. G. Giambastiani*
Institute of Chemistry and Processes for Energy,
Environment and Health (ICPEES),
ECPM, UMR 7515 of the CNRS and
University of Strasbourg,
25 rue Becquerel, 67087 Strasbourg Cedex 02, France.

Supporting information for this article is available on the WWW under https://doi.org/10.1002/slct.202203560

Special Collection *Part of the "DCO-SCI Prize and Medal Winners 2020/2021" Special Collection.*

higher number of structural defects and a reduced N-loading. Consequently, their CO_2 uptake capacity is moderate, especially at ambient conditions.[15–16]

In this paper, we report the synthesis of a new covalent triazine framework (**CTF-Napht**) prepared under ionothermal conditions from a 2,6-Dicyano-1,5-naphthyridine (**4**) building block. The high N/C ratio of the newly designed dinitrile together with the employ of relatively low synthetic temperatures (600 °C) have led to a well-performing material able to reach high levels of CO_2 adsorption at room conditions (1 bar, 298 K). Despite its moderate SSA (1341 m^2/g), **CTF-Napht** outperforms many CTF materials from the literature with more than doubled surface areas. The high thermodynamic affinity of **CTF-Napht** towards CO_2 is also highlighted by its remarkable isosteric heat of adsorption at zero coverage (Q_{st} = 39.6 KJ mol^{-1}) that ranks among the highest reported so far for this class of materials.

Results and Discussion

Synthesis and characterization

2,6-Dicyano-1,5-naphthyridine (**4**) (the building block for **CTF-Napht** synthesis) has been prepared following slightly modified literature procedures, as summarized on Scheme 1.

1,5-naphthyridine (**2**) has been prepared according to a Skraup-like protocol.[17–18] Dehydrated glycerol underwent a nucleophilic attack by 3-amino-pyridine (**1**) with subsequent acid-catalyzed ring closure and oxidation by means of iodine obtaining **2** in good yield as a white solid. After chromatographic purification, **2** was treated with *m*-chloroperbenzoic acid to get the corresponding di-N-oxide counterpart (**3**) as a yellow solid (82% yield).[19] The latter was finally treated with an acyl chloride and trimethylsilyl cyanide to afford **4** through a rapid and efficient multicomponent naphtiridine core functionalization reaction.[20,21] The target dicyano building block **4** was therefore obtained in one-pot from **3** in good yield (76%) as a white solid and further exploited for CTF synthesis. **CTF-Napht** was prepared from **4** under classical ionothermal conditions[5] in molten $ZnCl_2$ through a cyclotrimerization reaction. In this type of synthesis, Zinc chloride is known to have a triple function as reaction medium, Lewis acid trimerization catalyst and porogen agent and it is commonly used in large excess.[5] Accordingly, **4** was mixed with dry $ZnCl_2$ (1:5 molar ratio) in a glove-box and the resulting mixture sealed under vacuum into a quartz ampule before being heated at 600 °C for 20 h (see experimental section for details). After careful purification, **CTF-Napht** was finally recovered as a highly porous and amorphous black solid featured by a layered-structured morphology as can be argued from SEM analysis (Figure S1). Infrared (IR) spectroscopy highlights the complete trimerization of the monomer **4**, with no residual nitrile groups ($\approx$2300 cm^{-1}) present in **CTF-Napht** (Figure S2).

The N_2 adsorption isotherm collected on **CTF-Napht** and the relative micropore size distribution are shown on Figure 1A. As previously found for dicyano-building blocks bearing pyridinic functionalities,[13] **CTF-Napht** shows a type-I isotherm profile typical of microporous materials. This morphological feature is ascribed to an intimate Lewis acid-base interaction between the pyridinic moieties and $ZnCl_2$ that brings a more dense coordination geometry throughout the cyclotrimerization process.[8] As a result, **CTF-Napht** shows a satisfactory Specific Surface Area (SSA) of 1341 $m^2 g^{-1}$ together with a total pore volume of 0.685 $cm^3 g^{-1}$ (V_{micro} = 0.605 $cm^3 g^{-1}$, 90%). The micropore size distribution calculated through NL-DFT and assuming a slit-like pore shape (typical of carbonaceous materials) reveals the presence of (large) micropores in the 23–25 Å size range (Figure 1A'), at the border between micropores and mesopores. Several literature precedents remark the central role played by micropores (by a high V_{micro}/V_{tot} ratio in particular) on the material ability to efficiently adsorb CO_2.[22–24] Thus, **CTF-Napht** is a promising material for CCS applications. On the other hand, N-content and more specifically basic N-moieties are commonly recognized as preferential adsorption sites for CO_2.[25] The choice of a naphtiridine core together with controlled synthetic conditions (*i.e.* prolonged cyclotrimerization times at 600 °C) allowed to reach both goals, obtaining a highly microporous and N-rich polymer. It is well known that high synthetic temperatures (750-800 °C) ensure high SSA values but also partial carbonization accompanied by C–N cleavages and in turn materials pauperization in nitrogen.[13,16] The highly N-rich dicyano building block **4** together with a medium trimerization temperature represent an ideal compromise bringing to **CTF-Napht** with considerable SSA and N-loading as high as 14.9 wt.% as measured from CHN elemental analysis.

XPS analysis was finally carried out to get additional characterization of **CTF-Napht**. The survey spectrum reported on Figure S3 is in line with the expected material composition and confirms the complete removal of $ZnCl_2$ coming from the

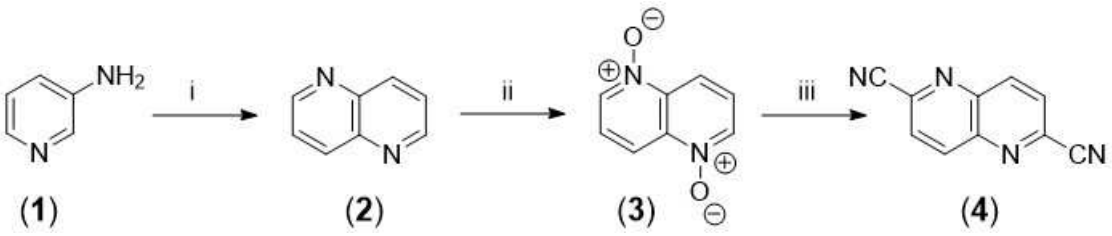

Scheme 1. Synthesis of 2,6-Dicyano-1,5-naphthyridine (**4**). Reagents and conditions: i) glycerol, conc. H_2SO_4, 0 °C; I_2, dioxane/water (1:1), reflux, overnight; ii) ClPhCOOOH, CH_2Cl_2/MeOH, rt, 72 h; iii) PhCOCl, Me_3SiCN, CH_2Cl_2, 40 °C, 2 h, isolated yield: 76%.

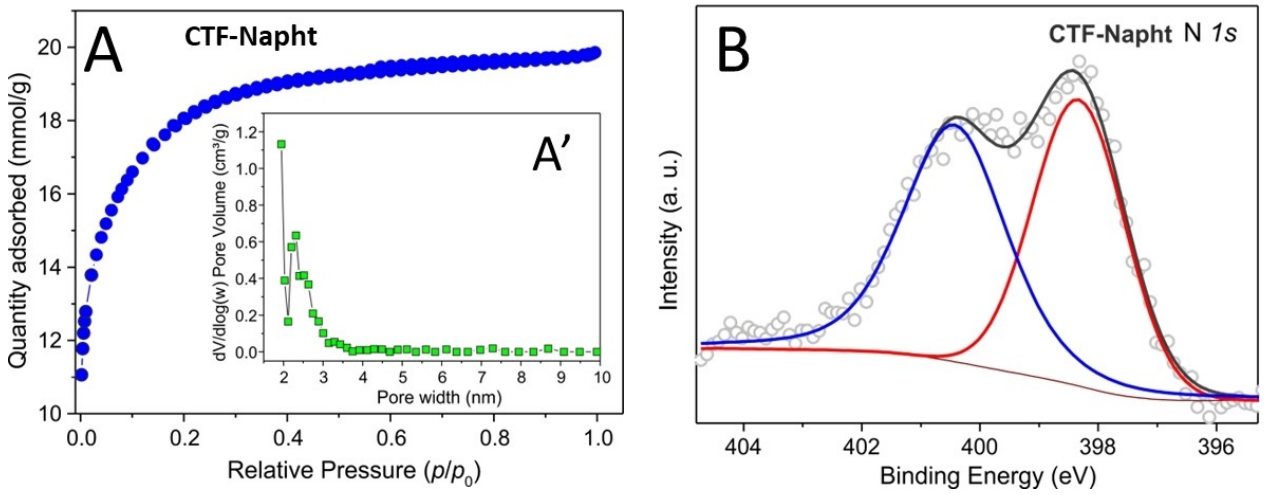

Figure 1. (**A**) N_2 adsorption-desorption isotherms recorded at 77 K for **CTF-Napht** together with relative micropore size distribution (**A'**) measured through NL-DFT method (slit-like pores). (**B**) High resolution N1s XPS analyses recorded on **CTF-Napht**.

synthesis. The high resolution N 1s XPS signal (Figure 1B) shows the absence of the starting –C≡N functional groups present in **4** and the typical profile of covalent triazine frameworks that can be conveniently fitted with two components at 398.3 and 400.4 eV commonly ascribed to pyridinic and pyrrolic nuclei, respectively.[13,26] While the former are likely due to N atoms of the triazine ring, the latter are generated by the thermal rearrangement of the material during the synthetic procedure.[27]

CO_2 adsorption properties

The high N-content together with a marked microporous character make **CTF-Napht** a good candidate for CCS applications. Accordingly, low pressure CO_2 adsorption isotherms were recorded at 252, 273 and 298 K (Figure 2) and results are summarized on Table 1. **CTF-Napht** shows a room temperature CO_2 uptake as high as 3.93 mmol/g (17.3 wt.%) at 1 bar, ranking among the covalent triazine frameworks with the highest adsorption capacity. As it can be argued from Table 1, with the only exception of high SSA CTF-py^{HT} [13] and TCNQ-CTF-700[28] prepared at higher trimerization temperatures (700–750 °C), the ultra-nanoporous HAT-CTF[29] and defluorinated materials,[30–31] **CTF-Napht** largely outperforms many benchmark and recently reported CTF materials from the literature. Worthy of note, the room temperature CO_2 adsorption capacity of **CTF-Napht** is higher than that reached by samples with markedly higher SSA values [*i.e.*, *bipy*-CTF600 (2479 m^2/g),[15] caCTF-1-700 (2367 m^2/g),[32] MM2 (1935 m^2/g),[33] F-DCBP-CTF-1 (2437 m^2/g),[26] CTF-*p*DCB/DCl^{HT} (3201 m^2/g),[16] DDP600 (2275 m^2/g)[34] *vs.* **CTF-Napht** (1341 m^2/g)], thus highlighting its strong affinity towards the target gas. In addition, **CTF-Napht** shows interesting CO_2 adsorption properties also at low pressure values. With a CO_2 uptake registered at 0.15 bar of 1.75 and 1.05 mmol/g at 273 and 298 K, respectively (Table 1),

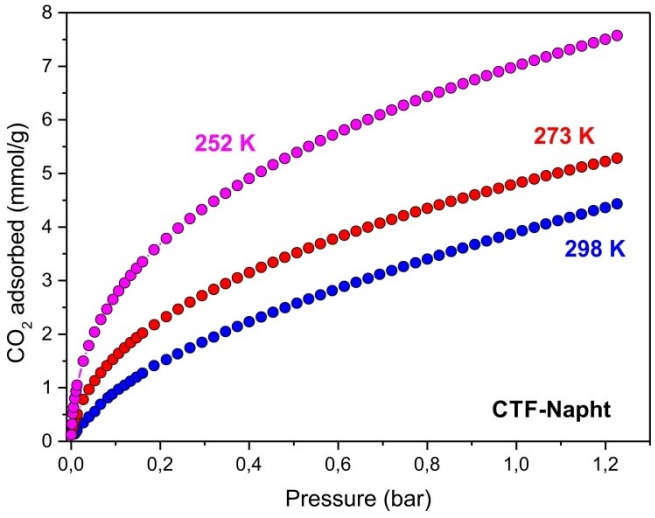

Figure 2. CO_2 adsorption isotherms registered for **CTF-Napht** at 252, 273 and 298 K

it overcomes the corresponding values registered for the high SSA CTF-py^{HT} [13] and fluorinated F-CTF-1-600.[25]

To get additional insight on the interaction strength with CO_2, the isosteric heat of adsorption (Q_{st}) was calculated on the basis of the Clausius-Clapeyron equation from isotherms measured at 252, 273 and 298 K (see Experimental section for details). This parameter is commonly recognized as an indicator of the thermodynamic affinity of materials for a target gas to be adsorbed. Q_{st} calculated for **CTF-Napht** has been found to be as high as 39.6 KJ mol^{-1} at zero coverage (Figure S4), representing one of the highest values reported so far for covalent triazine frameworks (Table 1).[6,10, 12] As a matter of fact, the cyano-building block design together with the judicious choice of trimerization conditions have boosted **CTF-Napht** to the boundary of the thermodynamics for CO_2 physisorption. 40 KJ mol^{-1} is indeed recognized as the upper limit for CO_2

Table 1. CO_2 adsorption uptake, Q_{st} and CO_2/N_2 selectivity values measured for **CTF-Napht** at comparison with the most representative and recently reported CTF systems from literature.

Materials	SSA (cm^3/g)	CO_2 uptake @1 bar [0.15 bar] (mmol/g) 273 K	298 K	Q_{st} ($KJ\,mol^{-1}$)[a]	CO_2/N_2 Selectivity[b]	Ref.
CTF-Napht	1341	4.84 [1.75]	3.93 [1.05]	39.6	42	this work
CTF-py^{HT}	3040	5.97 [1.04][c]	4.22 [0.61][c]	27.1	29	[13]
CTF-py	1239	5.08 [2.03][c]	3.79 [1.12][c]	35.1	45	
F-CTF-1-600	1535	5.53 [1.40][c]	3.41 [0.68][c]			[25]
CTF4	784	4.39 [1.51][c]	3.83 [1.23][c]	21.5	75	[14]
fl- CTF350	1235	4.28	2.29	32.7	27	[36]
bipy-CTF600	2479	5.58	2.95	34.4	37	[15]
HAT-CTF-450/600	1090	6.3 [3.0]	4.8 [2.0]	27.1	126	[29]
caCTF-1-700	2367	6.00	3.55	30.6		[32]
PHCTF-4	1270	2.34	1.57		40	[22]
CTF-20-400	1458	3.48	2.09	22	19	[37]
CTF-BIB-1	1636	4.35	2.53			[38]
MM2	1935	4.70	3.08	32		[33]
cCTF-500	1247	3.02	1.82	43		[39]
CTF-HUST-3	807	3.16	1.82	33		[40]
F-DCBP-CTF-1	2437	5.98 [2.15]	3.82 [1.19]	33.1	31	[26]
acac-CTF-5-500	1556	3.30	1.97	28.6	46	[41]
df-TzCTF600	1720	6.79 [2.17]	4.60	34	21	[31]
Tz-df-CTF600	2106	7.65	5.08	20		[30]
HATN-CTF-2	1994	5.57	3.53	32.6	33 (46)[d]	[42]
isox-CTF-5-400	1683	4.92	2.86	29		[43]
CTF-N_6	1236	5.0	3.4	26	36	[44]
ICTF-SCN	1010	2.48	1.40		24.8	[45]
TCNQ-CTF-700	3574	5.36	4.13	30.6		[28]
TCNQ-CTF-500	1479	4.78	3.38	27.6		
Pyrene-CTF-10	819	5.10	2.82			[46]
BCK-CTF-Gly	1720	5.56	2.68	33.3	37	[47]
CTF-*p*DCB/DCI^{HT}	3201	5.38	3.03	32.2	10	[16]
CTF-TPM-500	1206	2.74	1.68	29.8		[48]
TPP-CTF-4	1390	6.83	4.11		19	[49]
An-CTF-20-500	700	5.25	2.69			[50]
Py-CTF-400	1515	4.68	3.39	25.9		[51]
DDP600	2275	3.50	2.00	29.7		[34]
Pz-CTF6	1009	–	2.47			[52]
PTPOF-400–15		1.76	–			[53]

[a] at zero coverage; [b] evaluated on the basis of Henry model; [c] at 0.1 bar; [d] at 273 K

reversible physisorption involving Van der Waals forces,[16,31] while $Q_{st} > 40\ KJ\,mol^{-1}$ are typical values associated to chemisorption phenomena (such as those typically found for CO_2 aqueous amines solutions).[35]

Competitive CO_2 uptake over N_2 is an important parameter for practical applications as CO_2 adsorbent from post-combustion flue gases mixtures typically containing about 15% of CO_2 *vs.* 75% of N_2.[15] To this purpose, **CTF-Napht** CO_2/N_2 selectivity has been evaluated on the basis of the Henry model taking into account the initial slopes of the corresponding isotherms recorded at 298 K (Figure S5). **CTF-Napht** showed a good selectivity value of 42 (Table 1). It can be inferred that its highly microporous nature and channel dimensions that better match with CO_2 dynamic radius ensure a higher kinetic selectivity for CO_2 over N_2 hence opening promising perspectives for an efficient separation of CO_2/N_2 mixtures.[54]

Conclusions

A novel covalent triazine framework has been synthesized under ionothermal conditions starting from 2,6-Dicyano-1,5-naphthyridine as building unit. The newly designed dinitrile monomer with its high N/C ratio together with selected trimerization conditions have led to the obtainment of a N-rich porous polymer with enhanced performance for CCS applications. **CTF-Napht** offered one of the highest CO_2 uptake capacities at ambient conditions reported so far for this class of materials, outperforming many CTFs from the literature featured by more than doubled SSA values. The remarkable affinity of **CTF-Napht** for CO_2 is further confirmed by its $(Q_{st})_{CO2}$ value, as high as 39.6 KJ/mol, that stands at the upper thermodynamic limit for physical adsorption.

Experimental Section

All reactions were performed using standard Schlenk procedures under dry nitrogen atmosphere. Solvents were purified through standard distillation techniques while commercially available start-

ing materials were used as received, unless otherwise stated. **2** and **3** were prepared following literature procedures,[18–19] while **4** was synthesized adapting a reported protocol.[21] In brief, a solution of **3** (0.65 g, 4 mmol) and trimethylsilyl cyanide (2.5 mL, 20 mmol) in dry and degassed CH_2Cl_2 (140 mL) was stirred at room temperature for 10 minutes before adding benzyl chloride (1.53 mL, 13.2 mmol) dropwise. The as-obtained mixture was stirred for further 110 min at 40 °C and then washed with water (2×0 mL), $NaHCO_3$ sat. (2× 50 mL) and brine (2×50 mL). After stirring on Na_2SO_4 to remove traces of water, the collected organic phases were concentrated *in vacuo* affording 2,6-dicyano-1,5-naphthyridine (**4**) as a white solid in 76% yield. ^{1}H-NMR characterization was consistent with literature.[14]

CTF-Napht was prepared under classical ionothermal conditions in molten $ZnCl_2$.[5] **4** (0.25 g, 1.39 mmol) was finely grinded with a five-fold excess of dry $ZnCl_2$ (0.95 g, 6.94 mmol) in a glove-box and transferred in a quartz ampule. The mixture was dried under vacuum overnight, the ampule flame-sealed and then heated at 600 °C for 20 h in a furnace. After cooling to room temperature, the ampule was carefully opened and the black solid recovered. The latter underwent sequential washing cycles (water, HCl 1 M, NaOH 1 M, water and finally THF) before being dried to constant weight. Yield: 78%.

Electron microscopy images were acquired using a Tescan GAIA 3 FIB/SEM, at the CeME electron microscopy facility (CNR-ICCOM, Florence). For the sample preparation, a spatula tip of the powder was dropped on a stub covered by adhesive SEM tape. Excess (unadhered) sample was then removed by applying a gentle flux of Ar on the surface of the stub. The as-prepared sample was analyzed without further conductive coating, using an e-beam energy of 10 keV. *FT-IR spectroscopy* was performed on a PerkinElmer Spectrum BX FT-IR spectrophotometer in the 400–4000 cm^{-1} range with a resolution of 1 cm^{-1}. Samples were prepared mixing 2–3 wt.% of the material with spectroscopic grade KBr. *X-ray Photoelectron Spectroscopy (XPS)* analyses were performed under ultra-high vacuum (10^{-9} mbar) in a system equipped with a VSW HAC 5000 hemispherical electron energy analyzer and a non-monochromatized Mg–Kα X-ray source (1253.6 eV). Survey spectra were acquired at a pass energy of 44 eV (step size 1 eV) while high resolution spectra for detailed Binding Energy (BE) chemical shift analysis were registered at a pass energy of 22 eV with a step size of 0.05 eV. Spectra were calibrated on the sp^2 graphitic component of the C 1s spectrum (BE = 284.7 eV) and fitted with mixed Gaussian-Lorentzian peaks. *Elemental analyses* were conducted on a Thermo FlashEA 1112 Series CHNS–O instrument and elemental wt.% was calculated as average value over three independent runs. *Gas adsorption measurements.* N_2 adsorption isotherm was measured at 77 K on an ASAP 2020 Micromeritics instrument after degassing the sample at 200 °C for 12 h. The specific surface area (SSA) was determined on the basis of the Brunauer-Emmett-Teller (BET) method in the 0.1–0.22 p/p0 range (Figure S6). The micropore size distribution is reported as dV/dlog(W) *vs.* pore width (W) and was calculated assuming slit-like pores by using the NLDFT(SD3), N_2-77-Carbon Slit Pores DFT method provided by Micromeritics. Total pore volume was determined at 0.98 relative pressure. CO_2 adsorption isotherms were recorded up to 1.2 bar at 298, 273 and 252 K in order to extrapolate the carbon dioxide isosteric heat of adsorption (Q_{ads}) applying the differential form of the Clausius-Clapeyron equation:

$$\left[\frac{\partial(lnp)}{\partial\left(\frac{1}{T}\right)}\right]_{\theta} = -\frac{Q_{st}}{R}$$

where R is 8.315 $JK^{-1}mol^{-1}$. N_2 adsorption at 298 K up to 1.2 bar was also recorded for CO_2/N_2 selectivity evaluation on the basis of the Henry model, taking into account the initial slopes of the corresponding adsorption isotherms.[15]

Supporting Information Summary

SEM images, Infrared, survey XPS spectra for **CTF-Napht** together with Q_{st}, Henry and BET linear plots are provided in the Supporting Information.

Acknowledgements

TRAINER project (Catalysts for Transition to Renewable Energy Future) of the "Make our Planet Great Again" program (Ref. ANR-17-MPGA-0017) the Italian MIUR through the PRIN 2017 Project Multi-e (20179337R7) "Multielectron transfer for the conversion of small molecules: an enabling technology for the chemical use of renewable energy" are kindly acknowledged for financial support to this work.

Conflict of Interest

The authors declare no conflict of interest.

Data Availability Statement

The data that support the findings of this study are available in the supplementary material of this article.

Keywords: Carbon Capture and Storage · CO_2 physisorption · Covalent Triazine Frameworks · Cyclotrimerization · Porous Organic Polymers

[1] A. M. Varghese, G. N. Karanikolos, *Int. J. Greenhouse Gas Control* **2020**, *96*, 103005.
[2] https://www.noaa.gov/.
[3] M. Bui, C. S. Adjiman, A. Bardow, E. J. Anthony, A. Boston, S. Brown, P. S. Fennell, S. Fuss, A. Galindo, L. A. Hackett, J. P. Hallett, H. J. Herzog, G. Jackson, J. Kemper, S. Krevor, G. C. Maitland, M. Matuszewski, I. S. Metcalfe, C. Petit, G. Puxty, J. Reimer, D. M. Reiner, E. S. Rubin, S. A. Scott, N. Shah, B. Smit, J. P. M. Trusler, P. Webley, J. Wilcox, N. Mac Dowell, *Energy Environ. Sci.* **2018**, *11*, 1062–1176.
[4] T. Spitz, V. Avagyan, F. Ascui, A. R. W. Bruce, H. Chalmers, M. Lucquiaud, *Int. J. Greenhouse Gas Control* **2018**, *74*, 296–311.
[5] P. Kuhn, M. Antonietti, A. Thomas, *Angew. Chem. Int. Ed.* **2008**, *47*, 3450–3453; *Angew. Chem.* **2008**, *120*, 3499–3502.
[6] S. Pourebrahimi, M. Pirooz, *Clean. Chem. Eng.* **2022**, *2*, 100012.
[7] M. Liu, L. Guo, S. Jin, B. Tan, *J. Mater. Chem. A* **2019**, *7*, 5153–5172.
[8] P. Kuhn, A. Thomas, M. Antonietti, *Macromolecules* **2009**, *42*, 319–326.
[9] D. Y. Osadchii, A. I. Olivos-Suarez, A. V. Bavykina, J. Gascon, *Langmuir* **2017**, *33*, 14278–14285.
[10] C. Krishnaraj, H. S. Jena, K. Leus, P. Van Der Voort, *Green Chem.* **2020**, *22*, 1038–1071.
[11] J. Artz, *ChemCatChem* **2018**, *10*, 1753–1771.
[12] J. Wang, L. Wang, Y. Wang, D. Zhang, Q. Xiao, J. Huang, Y.-N. Liu, *Chin. J. Chem. Eng.* **2022**, *42*, 91–103.

[13] G. Tuci, M. Pilaski, H. Ba, A. Rossin, L. Luconi, S. Caporali, C. Pham-Huu, R. Palkovits, G. Giambastiani, *Adv. Funct. Mater.* **2017**, *27*, 1605672.
[14] G. Tuci, A. Iemhoff, H. Ba, L. Luconi, A. Rossin, V. Papaefthimiou, R. Palkovits, J. Artz, C. Pham-Huu, G. Giambastiani, *Beilstein J. Nanotechnol.* **2019**, *10*, 1217–1227.
[15] S. Hug, L. Stegbauer, H. Oh, M. Hirscher, B. V. Lotsch, *Chem. Mater.* **2015**, *27*, 8001–8010.
[16] G. Tuci, A. Iemhoff, A. Rossin, D. Yakhvarov, M. F. Gatto, R. Balderas-Xicohténcatl, L. Zhang, M. Hirscher, R. Palkovits, C. Pham-Huu, G. Giambastiani, *Int. J. Hydrogen Energy* **2022**, *47*, 8434–8445.
[17] Z. Wang, in *Comprehensive Organic Name Reactions and Reagents* (Ed.: I. John Wiley & Sons), **2010**, pp. 2603–2608.
[18] M. Balkenhohl, R. Greiner, I. S. Makarov, B. Heinz, K. Karaghiosoff, H. Zipse, P. Knochel, *Chem. Eur. J.* **2017**, *23*, 13046–13050.
[19] F. J. R. Rombouts, J.-I. Andrés, M. Ariza, J. M. Alonso, N. Austin, A. Bottelbergs, L. Chen, V. Chupakhin, E. Cleiren, K. Fierens, A. Fontana, X. Langlois, J. E. Leenaerts, J. Mariën, C. Martínez Lamenca, R. Salter, M. E. Schmidt, P. Te Riele, C. Wintmolders, A. A. Trabanco, W. Zhang, G. Macdonald, D. Moechars, *J. Med. Chem.* **2017**, *60*, 1272–1291.
[20] D. Heulyn Jones, S. T. Kay, J. A. McLellan, A. R. Kennedy, N. C. O. Tomkinson, *Org. Lett.* **2017**, *19*, 3512–3515.
[21] A. N. Singh, R. P. Thummel, *Inorg. Chem.* **2009**, *48*, 6459.
[22] K. Yuan, C. Liu, L. Zong, G. Yu, S. Cheng, J. Wang, Z. Weng, X. Jian, *ACS Appl. Mater. Interfaces* **2017**, *9*, 13201–13212.
[23] A. Bhunia, I. Boldog, A. Möller, C. Janiak, *J. Mater. Chem. A* **2013**, *1*, 14990–14999.
[24] K. Yuan, C. Liu, J. Han, G. Yu, J. Wang, H. Duan, Z. Wang, X. Jian, *RSC Adv.* **2016**, *6*, 12009–12020.
[25] Y. Zhao, K. X. Yao, B. Teng, T. Zhang, Y. Han, *Energy Environ. Sci.* **2013**, *6*, 3684–3692.
[26] G. Wang, K. Leus, H. S. Jena, C. Krishnaraj, S. Zhao, H. Depauw, N. Tahir, Y.-Y. Liu, P. Van Der Voort, *J. Mater. Chem. A* **2018**, *6*, 6370–6375.
[27] K. Wang, H. Huang, D. Liu, C. Wang, J. Li, C. Zhong, *Environ. Sci. Technol.* **2016**, *50*, 4869–4876.
[28] Q.-W. Deng, G.-Q. Ren, Y.-J. Li, L. Yang, S.-L. Zhai, T. Yu, L. Sun, W.-Q. Deng, A. Li, Y.-H. Zhou, *Mat. Today Energy* **2020**, *18*, 100506.
[29] X. Zhu, C. Tian, G. M. Veith, C. W. Abney, J. Dehaudt, S. Dai, *J. Am. Chem. Soc.* **2016**, *138*, 11497–11500.
[30] S. Mukherjee, M. Das, A. Manna, R. Krishna, S. Das, *Chem. Mater.* **2019**, *31*, 3929–3940.
[31] S. Mukherjee, M. Das, A. Manna, R. Krishna, S. Das, *J. Mater. Chem. A* **2019**, *7*, 1055–1068.
[32] Y. J. Lee, S. N. Talapaneni, A. Coskun, *ACS Appl. Mater. Interfaces* **2017**, *9*, 30679–30685.
[33] S. Dey, A. Bhunia, H. Breitzke, P. B. Groszewicz, G. Buntkowsky, C. Janiak, *J. Mater. Chem. A* **2017**, *5*, 3609–3620.
[34] M. Mahato, S. Nam, R. Tabassian, S. Oh, V. H. Nguyen, I.-K. Oh, *Adv. Funct. Mater.* **2022**, *32*, 2107442.
[35] B. Dutcher, M. Fan, A. G. Russell, *ACS Appl. Mater. Interfaces* **2015**, *7*, 2137–2148.
[36] S. Hug, M. B. Mesch, H. Oh, N. Popp, M. Hirscher, J. Senkerd, B. V. Lotsch, *J. Mater. Chem. A* **2014**, *2*, 5928–5936.
[37] G. Wang, K. Leus, S. Zhao, P. Van Der Voort, *ACS Appl. Mater. Interfaces* **2018**, *10*, 1244–1249.
[38] J. Du, Liu, R. Krishna, Y. Yu, Y. Cui, S. Wang, Y. Liu, X. Song, Z. Liang, *ACS Appl. Mater. Interfaces* **2018**, *10*, 26678–26686.
[39] O. Buyukcakir, S. H. Je, S. N. Talapaneni, D. Kim, A. Coskun, *ACS Appl. Mater. Interfaces* **2017**, *9*, 7209–7216.
[40] K. Wang, L.-M. Yang, X. Wang, L. Guo, G. Cheng, C. Zhang, S. Jin, B. Tan, A. Cooper, *Angew. Chem. Int. Ed.* **2017**, *56*, 14149–14156; *Angew. Chem.* **2017**, *129*, 14337–14341.
[41] H. S. Jena, C. Krishnaraj, G. Wang, K. Leus, J. Schmidt, N. Chaoui, P. Van Der Voort, *Chem. Mater.* **2018**, *30*, 4102–4111.
[42] G. Wang, N. Tahir, I. Onyshchenko, N. De Geyter, R. Morent, K. Leus, P. Van Der Voort, *Microp. Mesop. Mater.* **2019**, *290*, 109650.
[43] H. S. Jena, C. Krishnaraj, J. Schmidt, K. Leus, K. Van Hecke, P. Van Der Voort, *Chem. Eur. J.* **2020**, *26*, 1548–1557.
[44] C. Liao, Z. Liang, B. Liu, H. Chen, X. Wang, H. Li, *ACS Appl. Nano Mater.* **2020**, *3*, 2889–2898.
[45] H. Zhu, W. Lin, Q. Li, Y. Hu, S. Guo, C. Wang, F. Yan, *ACS Appl. Mater. Interfaces* **2020**, *12*, 8614–8621.
[46] M. G. Mohamed, A. F. M. EL-Mahdy, Y. Takashi, S.-W. Kuo, *New J. Chem.* **2020**, *44*, 8241–8253.
[47] B. Dong, D.-Y. wang, W.-J. Wang, X.-L. Tian, G. Ren, *Microp. Mesop. Mater.* **2020**, *306*, 110475.
[48] Y. Zhao, H. Huang, H. Zhu, C. Zhong, *Microp. Mesop. Mater.* **2022**, *329*, 111526.
[49] K. Y. Lin, A. F. M. EL-Mahdy, *Mat. Chem. Phys.* **2022**, *281*, 125850.
[50] M. G. Mohamed, S. U. Sharma, N.-Y. Liu, T. H. Mansoure, M. M. Samy, S. V. Chaganti, Y.-L. Chang, J.-Y. Lee, S.-W. Kuo, *Int. J. Mol. Sci.* **2022**, *23*, 3174.
[51] Y. Chen, X. Hu, J. Guo, Z. Guo, H. Zhan, S. Du, *Eur. Polym. J.* **2022**, *171*, 111215.
[52] V. M. Rangaraj, K. S. K. Reddy, G. N. Karanikolos, *Chem. Eng. J.* **2022**, *429*, 132160.
[53] F. Liu, X. Duan, X. Dai, S. Du, J. Ma, F. Liu, M. Liu, *Chem. Eng. J.* **2022**, *445*, 136687.
[54] Y. Fu, Z. Wang, S. Li, X. He, C. Pan, J. Yan, G. Yu, *ACS Appl. Mater. Interfaces* **2018**, *10*, 36002–36009.

Submitted: September 12, 2022
Accepted: October 11, 2022

RESEARCH ARTICLE

The synthesis of a novel Covalent Triazine Framework based on 2,6-Dicyano-1,5-naphthyridine building unit has been carried out. The as prepared CTF-Napht demonstrated outstanding affinity towards CO_2 with remarkable carbon dioxide uptake capacity at ambient conditions and a high isosteric heat of adsorption value.

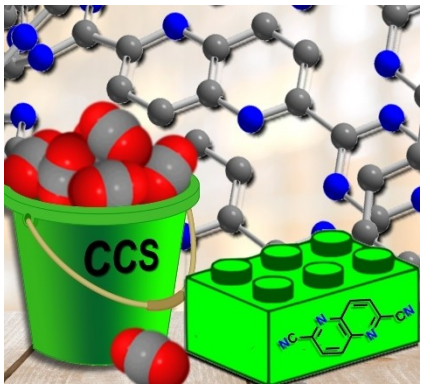

Dr. G. Tuci, M. Pugliesi, Dr. A. Rossin, Dr. C. Pham-Huu, Dr. E. Berretti, Dr. G. Giambastiani*

1 – 7

Design of a Novel Naphtiridine-based Covalent Triazine Framework for Carbon Dioxide Capture and Storage Applications